

14. Phase diagram of a spin glass of $\text{Eu}_p\text{Sr}_{1-p}\text{S}$

(桂 重俊) (松野 明)

Shigetoshi Katsura and Akira Matsuno

Department of Applied Physics,

Tohoku University, Sendai 980, Japan

Abstract

$\text{Eu}_p\text{Sr}_{1-p}\text{S}$ was modeled as a site-diluted Ising model with first and second neighbor interactions ($J>0$, $J'<0$) between Eu atoms, on the lattice with square coordination number z_c . By use of the reducibility of four-body density matrix to one-body density matrix, the integral equation for the distribution function for the effective field is obtained. The integral equation for the case $J'=-J/2$ is solved exactly at $T=0$ in the case of $z_c=2$ and the three solutions for paramagnetic, ferromagnetic, and the spin glass states are obtained. The boundary between the ferromagnetic and spin glass states is given by $p_{FG}=0.545$ and the phase diagram shows the reentrant behavior.

Recently $\text{Eu}_p\text{Sr}_{1-p}\text{S}$ attracted much attention as a material which shows the spin glass state [1]. In $\text{Eu}_p\text{Sr}_{1-p}\text{S}$, Eu or Sr atom locates at the lattice point of the face centered cubic lattice, and the exchange energies between Eu-Eu in the first and second neighbors are ferromagnetic and antiferromagnetic, respectively. We consider a model in which the magnetic ($m_i=1$, Eu, $\sigma_i=\pm 1$) or nonmagnetic ($m_i=0$, Sr) atom locates at the vertices on the cactus tree lattice as shown in Fig. 1. The effective field at the site i contributed from the outside of the site is denoted by $H_i^{(1)}$, that at the site i of the cluster $ijkl$ contributed from the inside of the cluster $ijkl$ is denoted by h_{i-ijkl} , and that at the site i of the cluster $ijkl$ contributed outside of the cluster $ijkl$ is denoted by $H_{i-ijkl}^{(4)}$. As seen Fig. 1, they are related by

$$\begin{aligned} H_i^{(1)} &= h_{i-ijkl} + H_{i-ijkl}^{(4)} \\ &= h_{i-ijkl} + h_{i-ij'k'l'} + \dots + h_{i-ij''k''l''} \end{aligned} \quad (1)$$

Then the one-body and four-body density matrices, $\rho^{(1)}$ and $\rho^{(4)}$, are given by

$$\rho^{(1)}(\sigma_i) = \exp(\beta H_i^{(1)} m_i \sigma_i) \quad (2)$$

$$\begin{aligned} \rho^{(4)}(\sigma_i, \sigma_j, \sigma_k, \sigma_l) &= \exp\left[\beta \sum_{\mu\nu} J_{\mu\nu} m_\mu m_\nu \sigma_\mu \sigma_\nu + \beta \sum_{\lambda\kappa} J'_{\lambda\kappa} m_\lambda m_\kappa \sigma_\lambda \sigma_\kappa \right. \\ &\quad \left. + \beta \sum_{\mu} H_{\mu-ijkl}^{(4)} m_\mu \sigma_\mu \right] \end{aligned} \quad (3)$$

where J and J' are the first neighbor ferromagnetic, and second neighbor antiferromagnetic exchange energies, respectively, and $\mu\nu$ and $\lambda\kappa$ denote first and second neighbor pairs, respectively. The distribution function $P(m_i)$ of m_i is given by

$$P(m_i) = p\delta(m_i - 1) + (1 - p)\delta(m_i) \quad (4)$$

where p is the concentration of the magnetic atoms (Eu).

We require the reducibility of density matrices as a self-consistent relation.

$$\frac{\rho_i^{(1)}}{\text{tr}\rho_i^{(1)}} = \frac{\text{tr}_{jkl}\rho_{ijkl}^{(4)}}{\text{tr}\rho_{ijkl}^{(4)}} \quad (5)$$

We consider the case where the site i is occupied by the magnetic atom, and hence $m_i = 1$. Then we have from (1),

$$h_{i-ijkl} = \frac{1}{2\beta} \ln \frac{f(1)}{f(-1)} \quad (6)$$

$$f(\sigma_i) = \sum_{\sigma_j \sigma_k \sigma_l} \exp(-\beta H_{i-ijkl}^{(4)} m_i \sigma_i) \rho^{(4)}(\sigma_i, \sigma_j, \sigma_k, \sigma_l) \quad (7)$$

The distribution functions of the effective fields

h_{i-ijkl} , $H_i^{(1)}$, $H_{i-ijkl}^{(4)}$ are denoted by $g_i(h)$, $G_i^{(1)}(H_i^{(1)})$, $G_i^{(4)}(H_{i-ijkl}^{(4)})$, respectively. Among the distribution functions $g_i(h)$, $G_i^{(4)}(H_{i-ijkl}^{(4)})$, the recurrence relation holds.

$$G_i^{(4)}(H_i^{(4)}) = \frac{1}{2\pi} \int dk \exp(ikH_i^{(4)}) [S(k)]^{z_c-1} \quad (8)$$

$$g_i(h_{i-ijkl}) = \int \delta(h_{i-ijkl} - \frac{1}{2\beta} \ln \frac{f(1)}{f(-1)}) \times \prod_{\mu=j,k,l} P(m_\mu) dm_\mu G_\mu^{(4)}(H_{\mu-ijkl}) dH_{\mu-ijkl} \quad (9)$$

where $S(k)$ is the Fourier transform of $g(h)$,

$$S(k) = \int \exp(-ikh) g(h) dh \quad (10)$$

and z_c is the number of squares connected at each vertex. We call it the square coordination number. In the case of fcc lattice, $z_c = 6$. In the uniform (paramagnetic, ferromagnetic, and spin glass) states, $g_i(h)$, and $G_i^{(4)}(H^{(4)})$ are considered not to depend on i , and the recurrence equation (8), (9) becomes an integral equation for $g(h)$ or $G(H^{(4)})$.

We consider the case $J'/J = -1/2$ and $T \rightarrow 0$. It is straight-forward but tedious to solve the integral equation for the case $z_c = 6$. We consider a simple model with $z_c = 2$. This simplified model of $\text{Eu}_p\text{Sr}_{1-p}\text{S}$ was considered by Katsura and Nagahara [2] [3]. They obtained the phase boundary between the paramagnetic and ferromagnetic states, and that between the paramagnetic and spin glass states. In this paper we give the boundary between the ferromagnetic and spin glass states of the same model which was not given in the previous paper. Since the effective field h_i at the site i is multiple of $J/2$ with maximum $5J/2$, we assume $g(h)$ as a superposition

of 11 δ -functions.

$$g(h) = \sum_{n=-5}^5 a_n (h - \frac{nJ}{2}) \quad (11)$$

In the case of the square cactus tree lattice $z_c = 2$, h_{i-ijkl} is equal to $H_{i-ij'k'l}^{(4)}$, and $g(h_i) = G(H_i^{(4)})$. In the limit $T \rightarrow 0$, the largest term in $f(1)$ and $f(-1)$ become dominant in (6), and hence we have

$$\begin{aligned} G(H^{(4)}) &= \sum_{mngm_jm_k m_1} a_m a_n a_q \\ &\times p^{m_j+m_k+m_1} (1-p)^{3-m_j-m_k-m_1} \\ &\times \delta(H^{(4)} - \frac{J}{2}(u_{mngm_jm_k m_1}(1) \\ &- u_{mngm_jm_k m_1}(-1))) \end{aligned} \quad (12)$$

where m, n, q run $-5, -4, \dots, 5$, m_j, m_k, m_1 run 0 and 1, and

$$\begin{aligned} u_{mngm_jm_k m_1}(\sigma_i) &= \max_{\sigma_j \sigma_k \sigma_l} [m_j \sigma_i \sigma_j + m_1 \sigma_l \sigma_i \\ &+ m_j m_k \sigma_j \sigma_k + m_k m_1 \sigma_k \sigma_l \\ &+ (-m_k \sigma_i \sigma_k - m_j m_1 \sigma_j \sigma_l + m m_j \sigma_j + n m_k \sigma_k \\ &+ q m_1 \sigma_l) / 2] \end{aligned} \quad (13)$$

Then (11) and (12) give 11 simultaneous equations for 11

unknowns (the number of total terms is 10648). These are polynomials generated by the formula manipulating system REDUCE. Using the normalization condition $\sum a_n = 1$ and noting* $a_{-5} = a_5 = 0$, we get 8 equations for 8 unknowns. We change the variable

$$\begin{aligned}
 v_e &= \frac{1}{2}(a_4 + a_{-4}) & v_o &= \frac{1}{2}(a_4 - a_{-4}) \\
 w_e &= \frac{1}{2}(a_3 + a_{-3}) & w_o &= \frac{1}{2}(a_3 - a_{-3}) \\
 x_e &= \frac{1}{2}(a_2 + a_{-2}) & x_o &= \frac{1}{2}(a_2 - a_{-2}) \\
 y_e &= \frac{1}{2}(a_1 + a_{-1}) & y_o &= \frac{1}{2}(a_1 - a_{-1}) \\
 z &= a_0 & & (14)
 \end{aligned}$$

and solve the equations by Newton-Raphson method and got three relevant solutions: the solution for the paramagnetic state (P), the ferromagnetic state (F), and the spin glass state (G).

* Two of the 11 equations obtained are

$a_{-5}(a_{-5}a_5p^3 - 1) = 0$ and $a_5(a_{-5}a_5p^3 - 1) = 0$. These equations cannot have the solutions such as $0 < a_{-5} < 1$ and $0 < a_5 < 1$.

They are characterized by

P: $z=1, v_e = w_e = x_e = y_e = 0$ central peaked δ -function

F: $v_o, w_o, x_o, y_o \neq 0$ asymmetric distribution

G: $v_o = w_o = x_o = y_o = 0$ symmetric distribution
 $v_e, w_e, x_e, y_e \neq 0$

The values of these amplitudes are shown in Figs. 3 and 4 as functions of the concentration of the ferromagnetic atoms. The concentration at which the ferromagnetic state disappears and connects to the spin glass state, p_{FG} , is obtained to be $p_{FG} = 0.545$. The boundary between the paramagnetic and ferromagnetic states and that between the paramagnetic and spin glass states were calculated in ref[2] and results for $J' = -J/2$ were given in Fig. 5 in ref [4]. [Ref [4] treated the spin glass in the dilute ferromagnet and dilute antiferromagnet.] The tricritical point there was $p_t = 0.488$. The phase diagram is shown in Fig. 5. It is compared with experimental phase diagram in Fig. 6 [1]. The reentrant behavior observed in the experiment was confirmed.

The appearance of the spin glass is due to the frustration as shown in Fig. 7. The frustration at the site i is a function of the concentration of the magnetic atom Eu and take maximum in some intermediate range ((b) in Fig. 7). Though the treatment for $z_c = 2$ simplified the fcc, the essential physical situation is realized in our model and gives a qualitative agreement with the

experiment.

Acknowledgments

The authors acknowledge helpful discussion with Professor R.Kikuchi, Professor S.Inawashiro, and Dr. S.Fujiki. The calculation were carried out by using the Computer Center of Tohoku University, in particular the REDUCE system.

References

- [1] H.Maletta and W.Felsch, Z.f.Phys. 37 55(1980).
- [2] S.Katsura and I.Nagahara, Z.f.Phys. 41,349(1980);
42,190(1981).
- [3] I.Nagahara, I.Hosaka and S.Katsura
[Comp.Phys.Commun,27,113(1982)] treated the same
problem in the octahedron approximation and got
similar results.
- [4] S.Katsura, S.Fujiki, T.Suenaga and I.Nagahara,
Phys.Stat.Sol.(b) 111 83(1982).

Figure Captions

- Fig. 1 Structure of $\text{Eu}_p\text{Sr}_{1-p}\text{S}$. ● denotes Eu^{2+} or Sr^{2+} and ○ denotes S^{2-} .
- Fig. 2 Square cactus tree lattice.
- Fig. 3 The amplitude of the distribution function $g(h)$ in
 (a) paramagnetic state, ^(p=0)
 (b) spin glass state, ^(p=0.43)
 (c) ferromagnetic state, ^(p=0.7)
 and (d) pure ferromagnetic
 (p = 1) state.
- Fig. 4 The values of v_e, w_e, x_e, y_e and v_o, w_o, x_o, y_o as functions of the concentration.
- Fig. 5 The phase diagram of the site-diluted Ising model on the square lattice, where $J' = -J/2 < 0$.
- Fig. 6 The phase diagram of $\text{Eu}_p\text{Sr}_{1-p}\text{S}$ in the experiment (Maletta and Felsch [1]).
- Fig. 7 Frustration at the site i of the cluster $ijkl$ for various concentration of magnetic atoms. ● denotes magnetic atom. (a) has weak frustration, (b) has strong frustration and (c), (d) and (e) have no frustration at the site i .

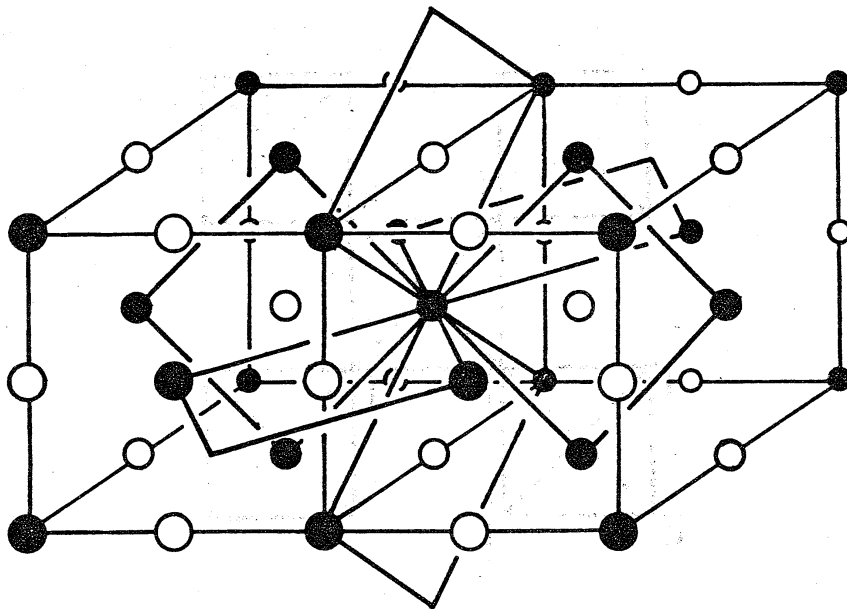


Fig. 1

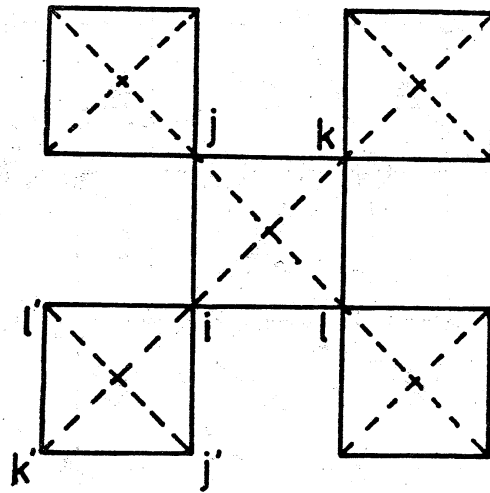
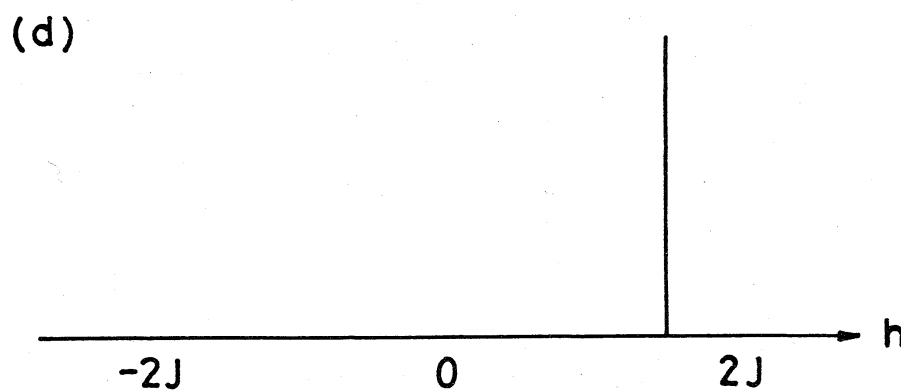
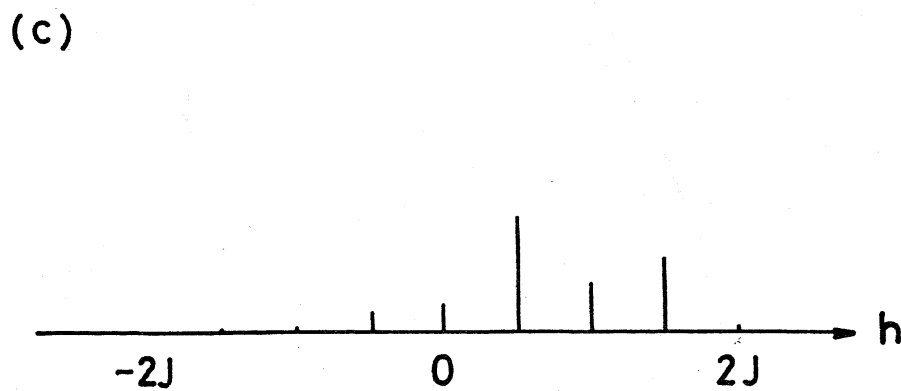
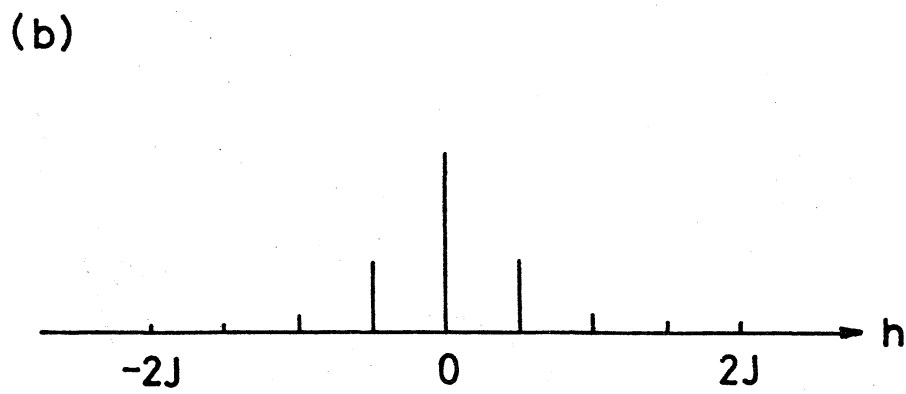
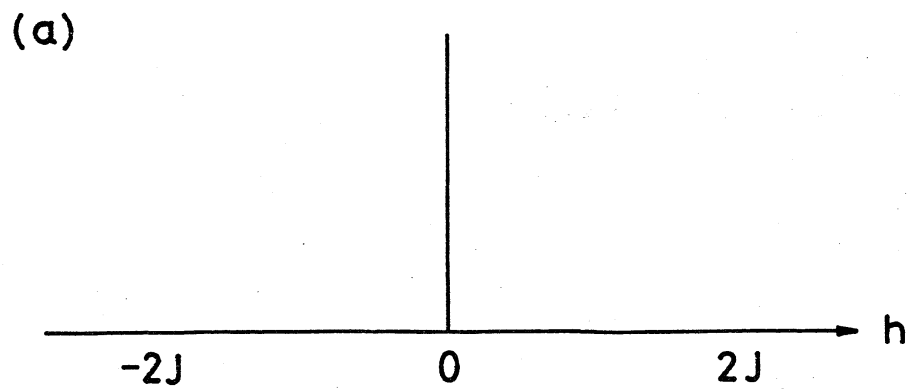


Fig. 2



(a)

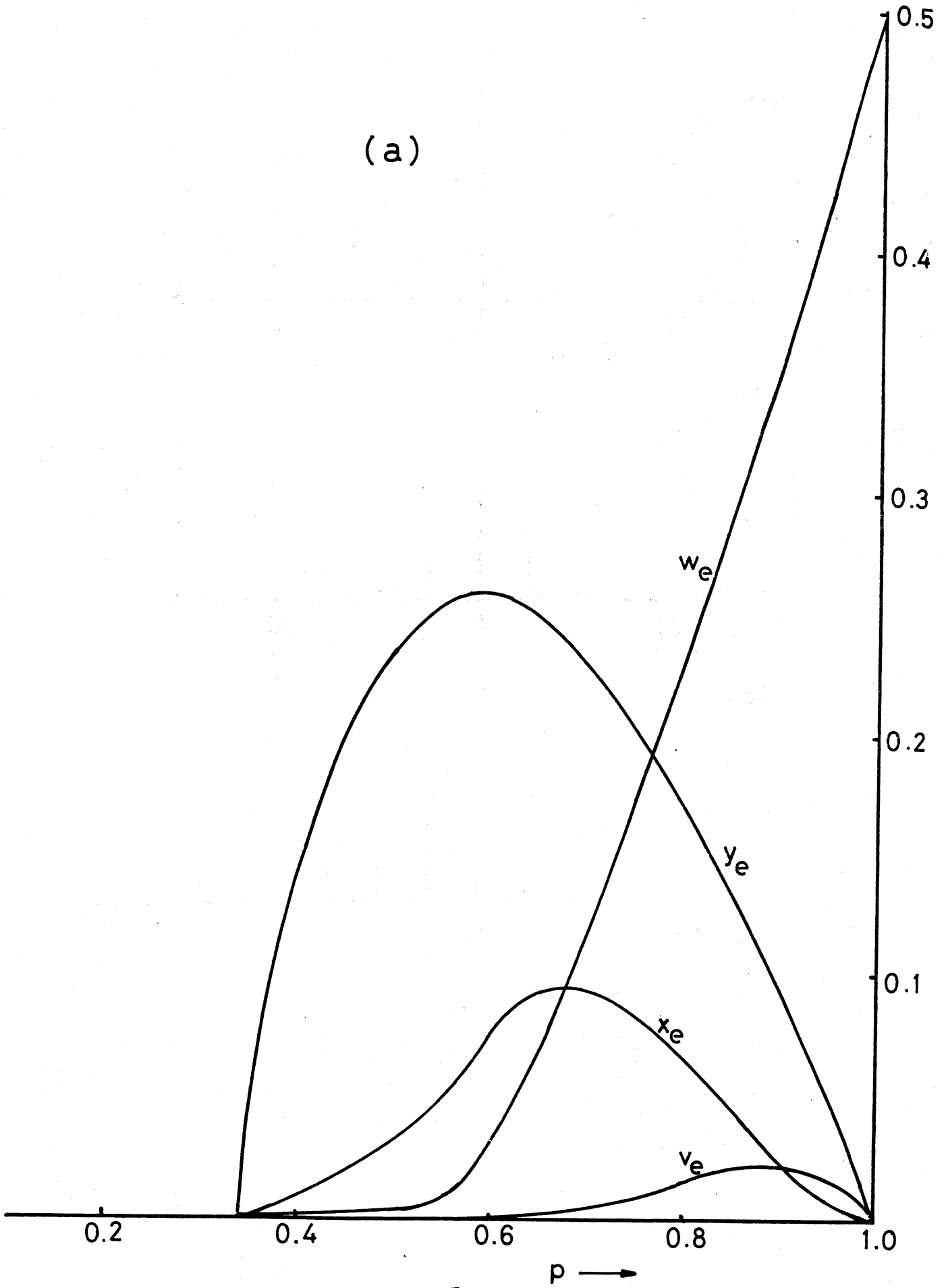
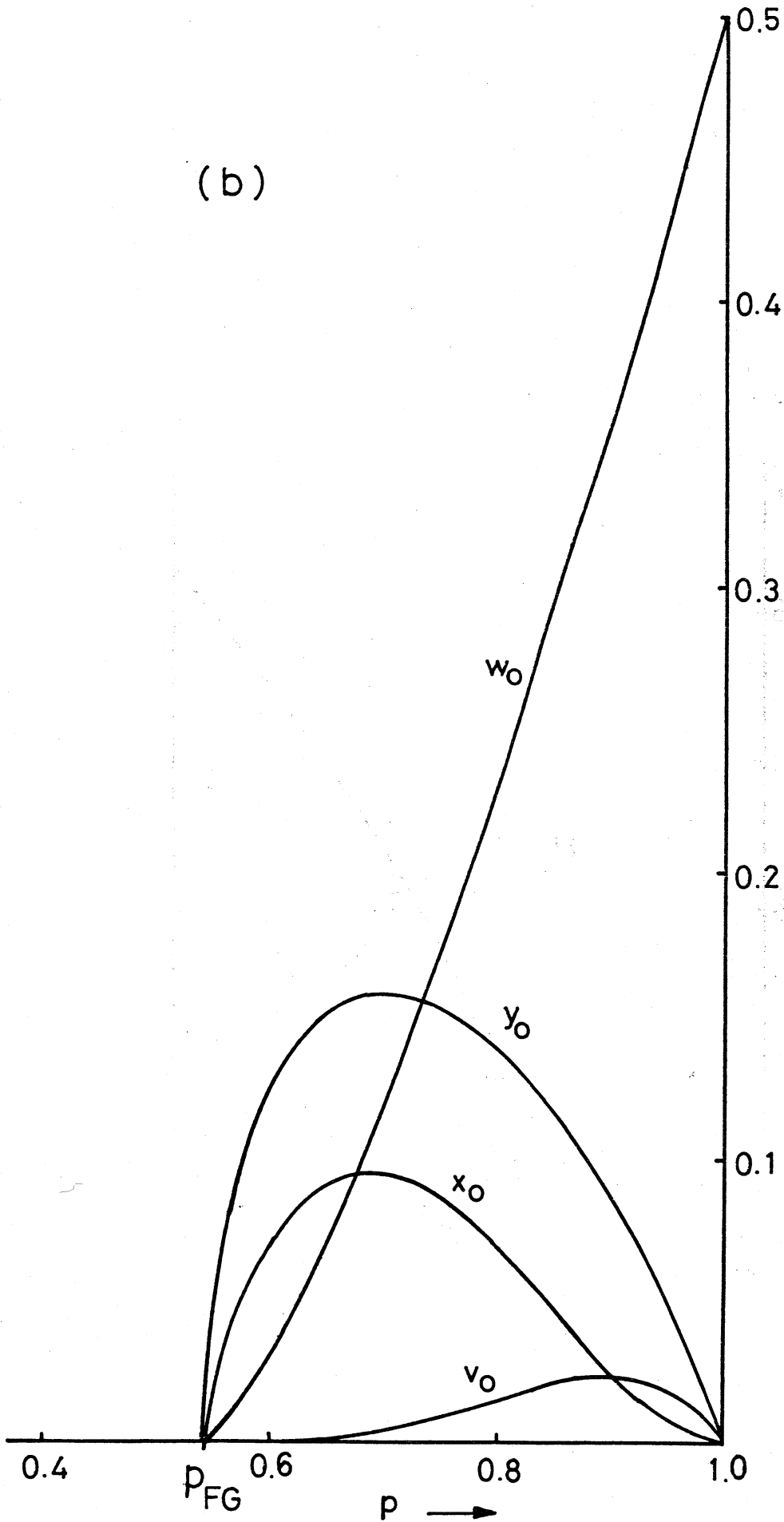


Fig. 7(b)

(b)



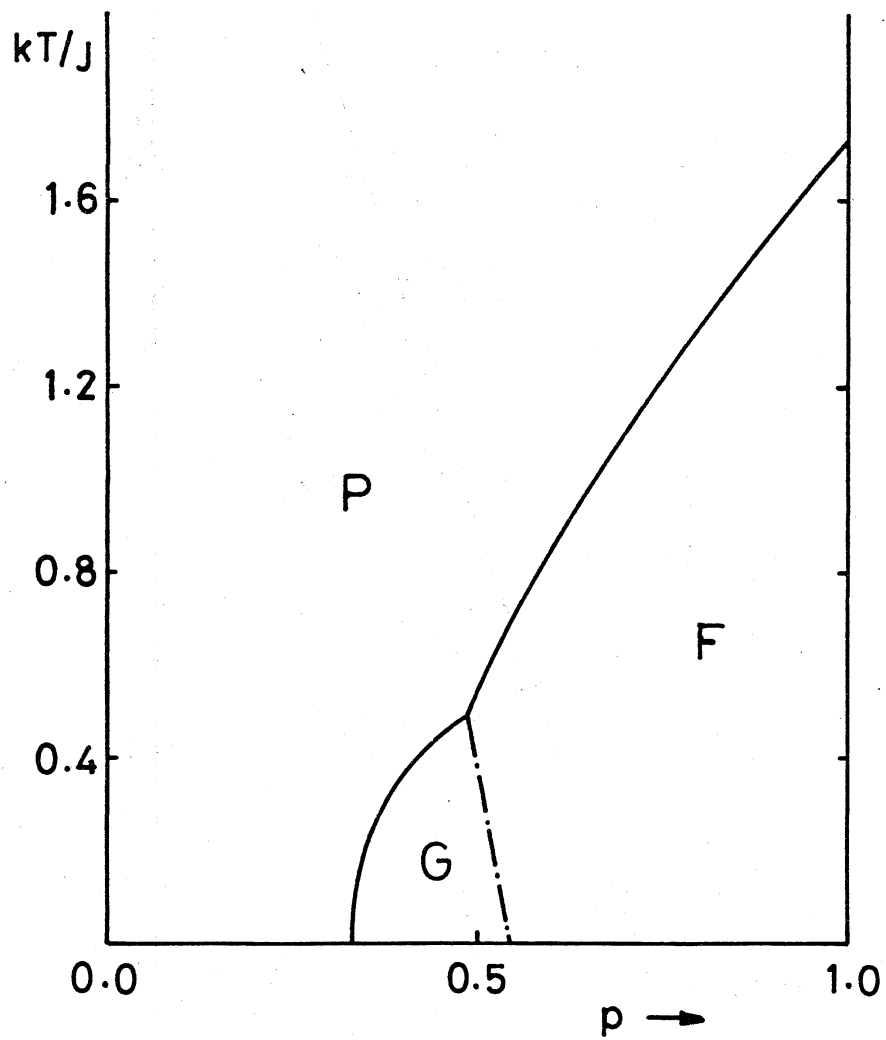


Fig. 5

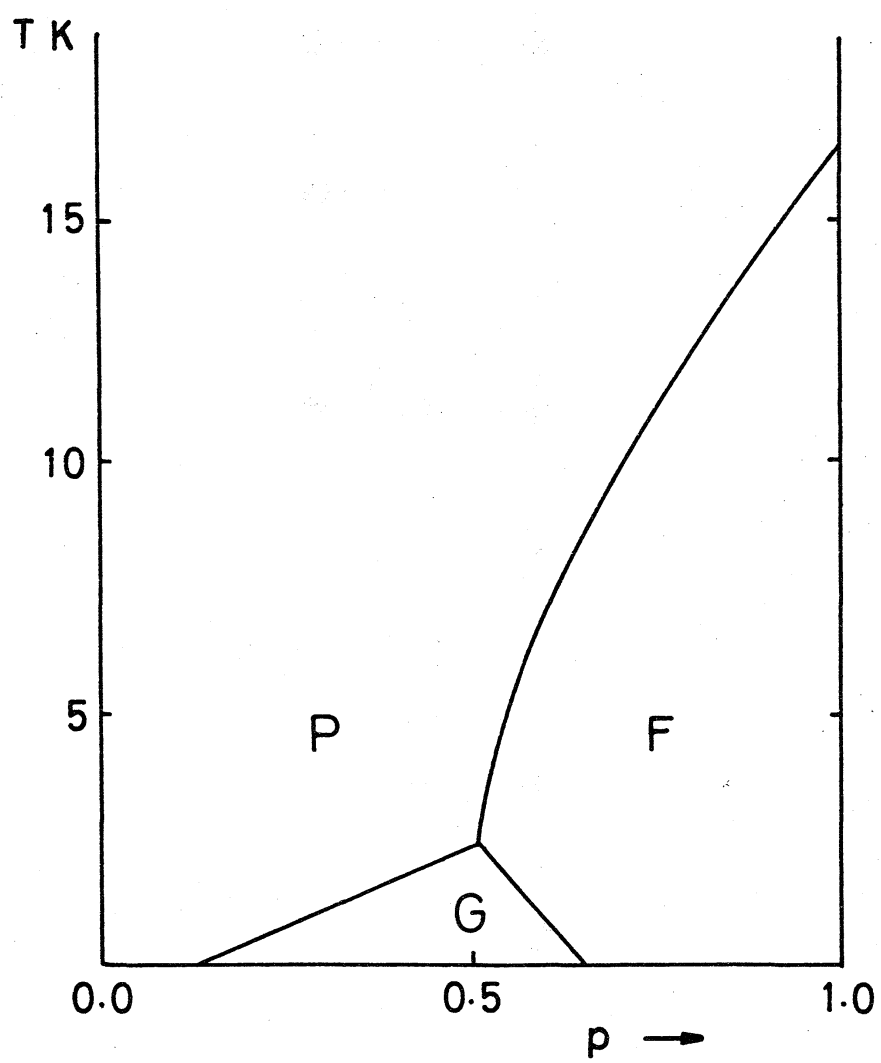


Fig. 6
18

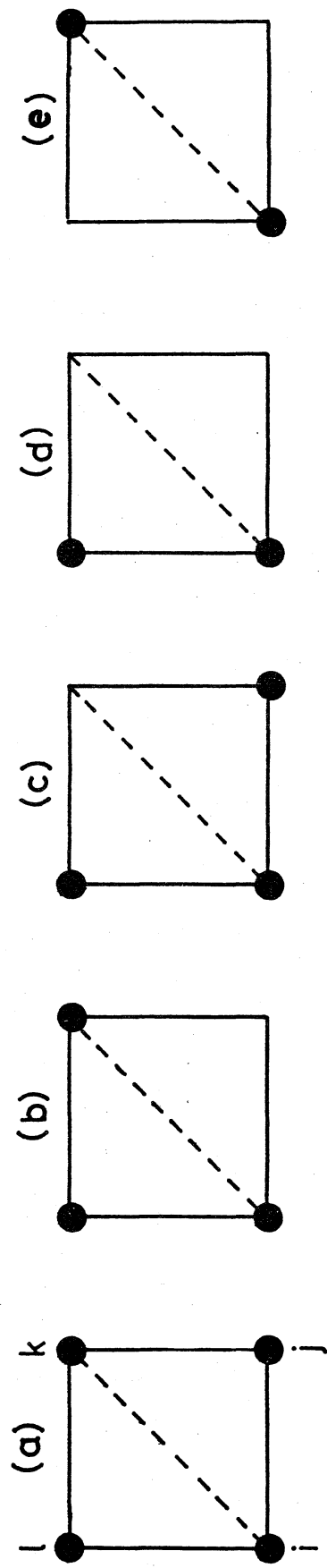


Fig. 7